Effective and Coupled Thermal Conductivities of Isotropic Open-Cellular Foams

J. G. Fourie
British Columbia Institute of Technology, Burnaby, BC, Canada V5G 3H2

J. P. Du Plessis
Dept. of Applied Mathematics, University of Stellenbosch, Private Bag X1, Matieland 7602, South Africa

The effective and the coupled thermal conductivity of the solid microstructure of open-cellular foams and an accompanying saturation fluid are defined in a conceptual representation of conductive heat transfer in a two-phase system of which the phases are in a thermal nonequilibrium state. The effective and coupled thermal conductivities were determined from a close observation of the relationship between microscopic and macroscopic temperature distributions. Temperature distributions were obtained from the numerical solution of the three-dimensional (3-D) conduction equation in a representative geometrical model of the foam solid microstructure and the fluid pores. Empirical correlations are provided for the effective and coupled thermal conductivities in terms of the solid and the fluid thermal conductivity and foam porosity. Thermal radiation was not considered in the energy transfer process. © 2004 American Institute of Chemical Engineers

AIChE J, 50: 547–556, 2004
Keywords: foam, heat transfer, effective thermal conductivity, coupled thermal conductivity, representative unit cell, mathematical modeling

Introduction

Rigid open-cellular foams made from a variety of metals, carbons, and ceramics have seen their introduction following advancement in manufacturing technologies on many fronts (Ashby et al., 2000; Banhart, 2000; Peng et al., 2000; Twigg and Richardson, 2002). Open-cellular foams are characterized by a consolidated solid microstructure composed of a series of interconnected ligaments capable of continuous thermal conduction. This, combined with a high specific surface area for heat exchange between the solid microstructure and a traversing saturation fluid, renders open-cellular foams, especially open-cellular metallic foams, suitable to act as an enhanced heat-transfer surface. Open-cellular foams have, therefore, seen an increase in application in recent years to enhance heat transfer in a variety of thermal devices, including adsorption heat pumps (Guilleminot and Gurgel, 1990), rocket liquid propellant combustion chambers (Fortini and Tuffias, 1998), and high power electronic devices (Antohe et al., 1996; Bastawros, 1998a; Lu et al., 1998a).

Thermal conductivity in open-cellular foams has been the subject of various experimental and analytical studies. An assumption of thermal equilibrium between the solid microstructure and the saturation fluid reduces the conceptual representation of thermal conduction at a macroscopic level to a single expression within a one-equation model, given in the mean conductive heat flow direction y denoted as (Nozad et al., 1985)

$$q_o = k_o \frac{\partial T_o}{\partial y} \tag{1}$$

The overall locally mean conductive heat flow is represented by $\boldsymbol{q_o}$, and $\partial T_o/\partial y$ represents the gradient in the locally mean

---

Correspondence concerning this article should be addressed to J. G. Fourie at jfourie@bcit.ca.

temperature, with a proportionality coefficient k_o referred to here as the overall thermal conductivity.

Various analytical models have been developed to predict the overall thermal conductivity k_o of a consolidated porous media, with some of them suited for application to open-cellular foams through the selection of a proper empirical geometry factor value (Tien and Vafai, 1979; Bauer, 1993; Hsu, 1994). Models developed specifically for open-cellular foams subjected to temperatures low enough to ignore the nonlinear effects of thermal radiation are limited to those of Dul'nev (1965), Schuetz and Glicksman (1984), Calmidi and Mahajan (1999), and Bhattacharya et al. (1999). Experimental data has been obtained for the overall thermal conductivities of open-cellular aluminum, nickel, and vitreous carbon (RVC) foams (Takegoshi et al., 1992; Calmidi and Mahajan, 1999; Bhattacharya et al., 1999; Paek et al., 2000).

Under certain conditions, the criteria for thermal equilibrium between the solid microstructure and the saturation fluid (Carbonell and Whitaker, 1984; Kim and Jang, 2002) requires for this assumption to be relaxed. Such conditions include the presence of internal heat generation (Sathe et al., 1990), heat-transfer augmentation from a wall surface where the foam attaches (Bastawros, 1998a; Calmidi and Mahajan, 2000), and foam systems in a thermal transient state (Hwang et al., 2002). Thermal conduction is then described at a macroscopic level by individual expressions for the solid microstructure and the saturation fluid in a two-equation model (Nozad et al., 1985). A number of macroscopic level intuitive two-equation model descriptions have been proposed in literature for porous media in general, according to which conduction in a phase is conceptually represented in terms of an effective phasial thermal conductivity, and the gradient of the locally mean temperature of that phase (Vortmeyer and Schaefer, 1974; Schlünder, 1975; Glatzmaier and Ramirez, 1988; Vafai and Sözen, 1990; Viskanta, 1995), given as

$$q_s = k_{ss}\frac{\partial T_s}{\partial y} \tag{2}$$

for the solid phase, and for the fluid phase, as

$$q_f = k_{ff}\frac{\partial T_f}{\partial y} \tag{3}$$

Here q_s and q_f are the locally mean conductive heat flow in the solid and the fluid phase, respectively, with k_{ss}, and k_{ff} referred to as the *effective thermal conductivity* of the solid and the fluid phase, respectively. The locally representative mean temperatures for the solid and the fluid phase are denoted as T_s and T_f, respectively .

Calmidi and Mahajan (2000) presented expressions for the effective thermal conductivity of the solid phase k_{ss}, and the fluid phase k_{ff} by, respectively, setting the thermal conductivity of the solid and the fluid phase equal to zero in their analytical expression for the overall thermal conductivity k_o.

The application of the analytical process of local volume averaging (Whitaker, 1967; Bear and Bachmat, 1986) to the microscopic energy equation has, however, shown that, in a thermal nonequilibrium state, conduction within a phase is not just a function of the gradient of the locally mean temperature of that phase, but also of the gradient of the locally mean temperature of the opposing phase (Carbonell and Whitaker, 1984; Nozad et al., 1985; Quintard and Whitaker, 1993; Kaviany, 1995). Conceptually, this finding is represented as

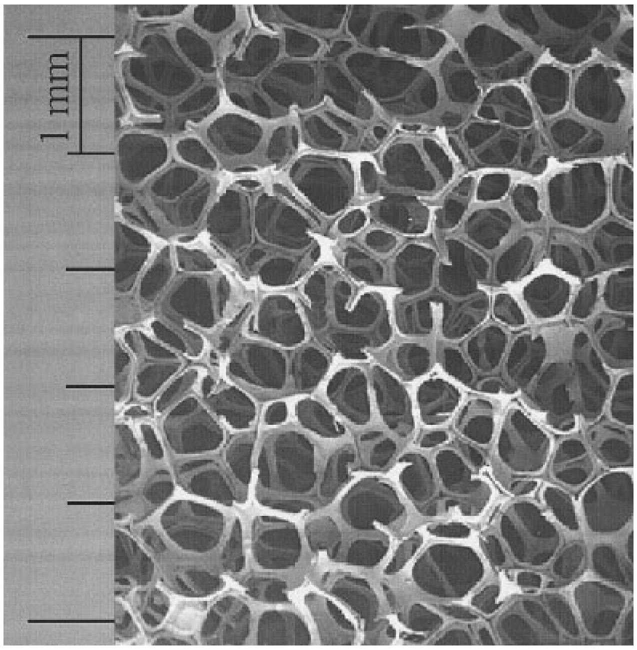

Figure 1. Open-cellular foam microstructure.

$$q_s = k_{ss}\frac{\partial T_s}{\partial y} + k_{sf}\frac{\partial T_f}{\partial y} \tag{4}$$

for the solid phase, and

$$q_f = k_{ff}\frac{\partial T_f}{\partial y} + k_{fs}\frac{\partial T_s}{\partial y} \tag{5}$$

for the fluid phase, where k_{sf} and k_{fs} are referred to as the *coupled thermal conductivity* of the solid and the fluid phase, respectively.

Various theoretical methods have been proposed to determine the effective and coupled thermal conductivities of the solid and the fluid phase of specific porous media and porous media in general (Carbonell and Whitaker, 1984; Whitaker, 1989; Quintard and Whitaker, 1993; Kaviany, 1995; Moyne, 1997; Hsu, 1999; Fourie and Du Plessis, 2003). Among these, the method proposed by Fourie and Du Plessis is unique in that it allows closure to be achieved with no constraints placed on length or timescales, and without the need to neglect terms of higher order in the analytical derivation. Furthermore, the method reduces to the classic one-equation model for the case of thermal equilibrium between the solid and the fluid phase.

An evaluation of the overall thermal conductivity k_o, the effective thermal conductivities k_{ss} and k_{ff}, and the coupled thermal conductivities k_{sf} and k_{fs} warrants an accurate descrip-

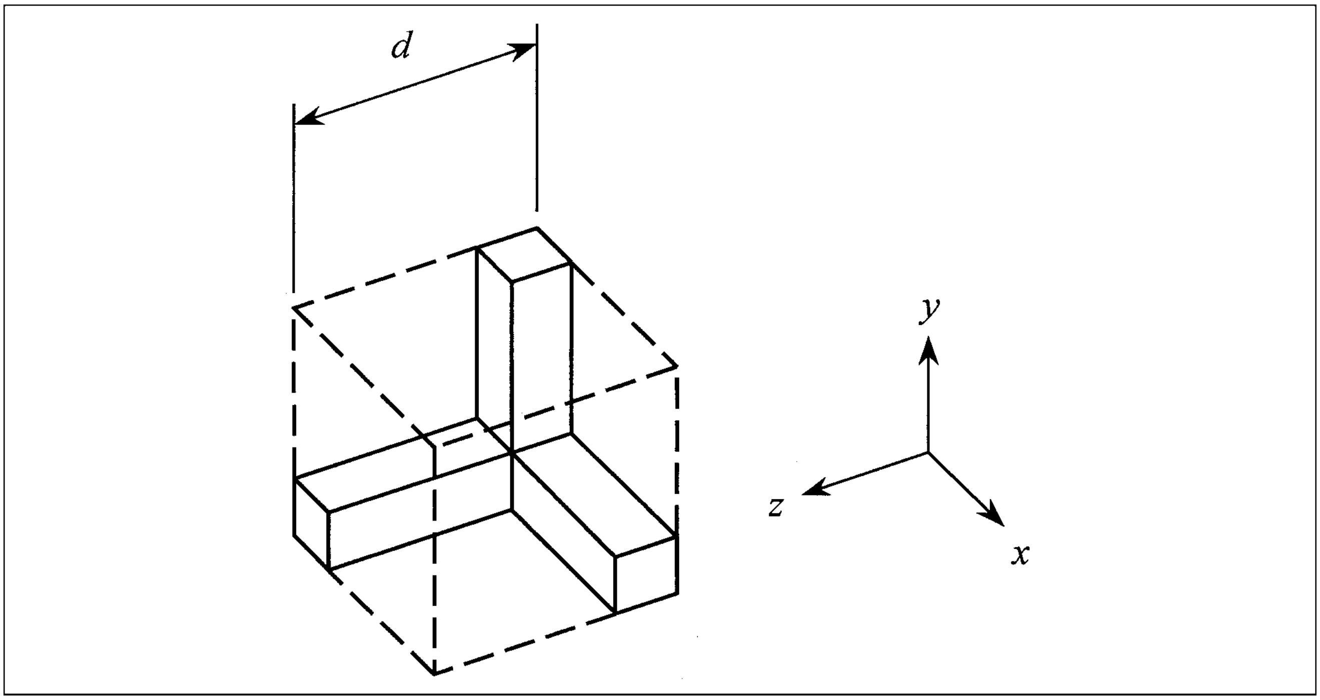

Figure 2. RUC for isotropic open-cellular foams.

tion of the foam morphology. Figure 1 shows the reticulated microstructure of an open-cellular ceramic foam. Although variations in the detail morphology occur between foams of different materials, open-cellular foams in general consist of duodecahedronally-shaped cells, with 12 to 14 pentagonal or hexagonal faces. Individual strands of triangular cross-sectional shape form the edges of the cells, with material clustering at the strand vertices. Although a close-up view shows complex intricate interfacial geometries, a more global view reveals a fair degree of uniformity. This has inspired a number of representative geometrical models in literature, such as cubic, tetrakaidecahedral, and 2-D hexagonal arrays of ligaments (Schuetz and Glicksman, 1984; Gibson and Ashby, 1988; Lu et al., 1998b; Bastawros et al., 1998b; Calmidi and Mahajan, 1999; Bhattacharya et al., 1999; Fourie and Du Plessis, 2002).

Dul'nev (1965) regarded open-cellular foam as an assembly of cubic units consisting of 12 solid square prisms. Mickley (Combarnous and Bories, 1975), and later Kamiuto (1997) rearranged the geometry of this model to consist of three mutually perpendicular solid square prisms, as shown in Figure 2. This model was later independently characterized, and after attributing various features to it, was introduced in literature as a *Representative Unit Cell* (RUC) for open-cellular foams (Du Plessis and Masliyah, 1988; Du Plessis, 1991).

Knowledge of the effective and coupled thermal conductivities of open-cellular foams is essential for the successful design and operation of high-performance thermal systems. Published accounts on efforts to determine these parameters through a method that is based on a rigorously derived two-equation model could not be found. This article is meant to fill that gap with the two-equation conduction model of Fourie and Du Plessis (2003), together with a representative geometrical model for open-cellular foams. Kamiuto (1997) and Paek et al. (2000) evaluated Dul'nev's rearranged geometrical model, and associated analytical expression for the overall thermal conductivity k_o of open-cellular foams, and found excellent agreement with experimental data. This, combined with its geometric simplicity, makes Dul'nev's rearranged model the choice for this study.

Analysis

Two-equation model

The two-equation model of Fourie and Du Plessis (2003) presents the effective and the coupled thermal conductivities, respectively as

$$k_{\gamma\gamma} \equiv \frac{k_{nd,\gamma}k_{e,\gamma} + \dfrac{\varepsilon_\varphi}{\varepsilon_\gamma} k_{nd,\varphi}k_{nd,\gamma}}{k_{nd,\gamma} + \dfrac{\varepsilon_\varphi}{\varepsilon_\gamma} k_{nd,\varphi}} \tag{6}$$

and

$$k_{\gamma\varphi} \equiv \frac{k_{nd,\varphi}(k_{e,\gamma} - k_{nd,\gamma})}{k_{nd,\gamma} + \dfrac{\varepsilon_\varphi}{\varepsilon_\gamma} k_{nd,\varphi}} \tag{7}$$

where $\gamma = s$ and $\varphi = f$, or *vice versa*. The respective volume fractions of the solid and the fluid phase within a *Representative Elementary Volume* (REV) are given by ε_s and ε_f. Details regarding the selection and conditions of an REV in a porous medium are outlined in Bear and Bachmat (1986). The equi-

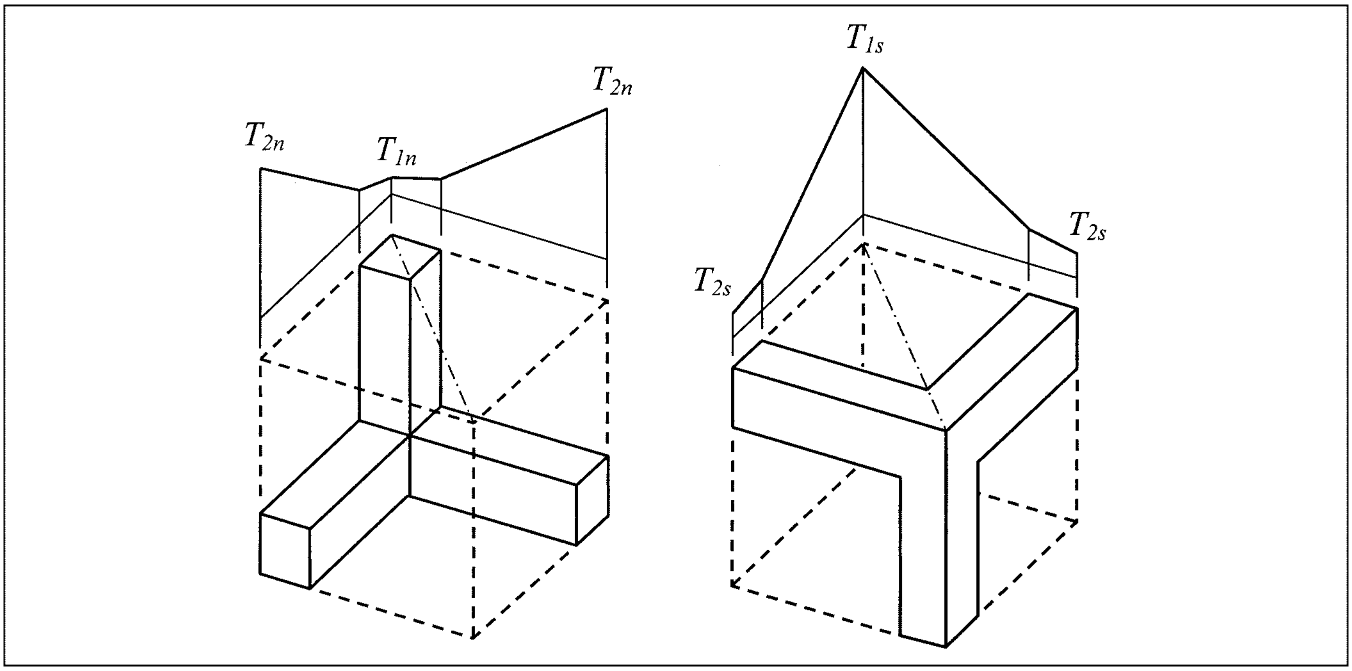

Figure 3. Northern and southern boundary temperature on the RUC.

librium thermal conductivity k_e, and the directional nonequilibrium thermal conductivity k_{nd}, are defined in a mean conductive heat flow direction y as

$$k_{e,\gamma} \equiv \frac{k_\gamma \displaystyle\int_{V_\gamma} \frac{\partial T_e}{\partial y}\, \mathrm{d}V}{\dfrac{\partial}{\partial y} \displaystyle\int_{V_\gamma} T_e \,\mathrm{d}V} \tag{8}$$

and

$$k_{nd,\gamma} \equiv \frac{k_\gamma \displaystyle\int_{V_\gamma} \frac{\partial T_{nd}}{\partial y}\, \mathrm{d}V}{\dfrac{\partial}{\partial y} \displaystyle\int_{V_\gamma} T_{nd} \,\mathrm{d}V} \tag{9}$$

where $\gamma = s$ or f. The respective solid and the fluid phase volume in the REV are given by V_s and V_f, and k_s and k_f are the solid and the fluid phase thermal conductivity. Furthermore, T_e and T_{nd} are characteristic microscopic temperature distributions referred to as the *equilibrium* and the *directional nonequilibrium* microscopic temperature distribution. These characteristic microscopic temperature distributions are defined in Fourie and Du Plessis (2003), and recapped here in Appendix A.

Geometrical model

Equations 6 to 9 suggest that the effective and coupled thermal conductivity of the solid and the fluid phase can be determined from an analysis of the characteristic microscopic temperature distributions T_e and T_{nd} in each phase, within an REV. With the RUC acting as a single cell representation of an REV, a feature of significance here is that the RUC for isotropic foam is rotationally invariant, and can be orientated with one of its principal axis parallel to the mean direction of conductive heat flow in a collocated REV. Because the RUC is rotationally invariant, an evaluation of the T_e and T_{nd} microscopic temperature distributions is only required in one of the principal directions. In this study, the analysis is done with reference to the y-direction in Figure 2.

Microscopic temperature distributions

The T_e and T_{nd} microscopic temperature distributions in the RUC are obtained from the computational solution of the energy equation in both phases. With steady-state conduction as the predominant means of heat transfer, and in the absence of heat sources (or sinks), the energy equation reduces to (Bird et al., 1960)

$$\nabla \cdot (k\nabla T) = 0 \tag{10}$$

The volume of the RUC, as shown in Figure 2, was divided into 8,000 (20 × 20 × 20) finite volumes of similar size and dimensions $\Delta x \times \Delta y \times \Delta z$ in the x, y, and z directions, respectively, with a grid point located at the center of each of the finite volumes. Equation 10 was discretized at each grid point with the method of Patankar (1980) to yield a set of simultaneous linear equations. With appropriate thermal conditions at the boundaries of the RUC, the temperature at each grid point was obtained from the solution of the set of simultaneous linear equations with the direct solution algorithm presented by King (1976).

A T_e microscopic temperature distribution, characterized by Eqs. A1 to A3, was induced within the RUC by, respectively, assigning two different arbitrarily selected uniform temperature distributions at the northern and southern boundaries of the RUC, whereas the boundaries normal to the x- and the z-directions are thermally insulated (zero heat flux). A T_{nd} microscopic temperature distribution, characterized by Eqs. A4 to A6, was induced with linear temperature distributions assigned in each phase at the northern and at the southern boundaries of the RUC, according to the arrangements shown in Figure 3. The linear temperature distributions apply from the edges where they are indicated in the figures, to the diagonal broken line (that is, the distributions have mirror images about a vertical plane intersecting the RUC at the broken lines). As in the previous case, the boundaries normal to the x- and the z-directions are thermally insulated.

The T_e and T_{nd} microscopic temperature distributions induced in this manner will not satisfy the conditions imposed by Eqs. A2 and A6. This is because the solid phase mass is not uniformly distributed within the RUC, that is, the solid phase center of mass does not coincide with the geometric center of the RUC. Although a uniform solid phase mass distribution is achievable by rearranging the three prisms of the RUC to intersect at the center of the RUC, it yields similar results than the RUC shown in Figure 2.

The gradients of the linear temperature distributions in Figure 3 are inversely proportional to the thermal conductivity of the corresponding phases. Temperatures $T_{1,n}$ and $T_{1,s}$ in Figure 3 were arbitrarily selected. Temperatures $T_{2,n}$ and $T_{2,s}$ were selected, such that from the computed T_{nd} temperature distribution, the discritized form of Eq. A4 is satisfied, that is

$$k_s \sum_{V_s} \left[\left(\frac{T_{nd,N} - T_{nd,P}}{\delta y_n} + \frac{T_{nd,P} - T_{nd,S}}{\delta y_s} \right) \Delta x \Delta y \Delta z \right] = -k_f \sum_{V_f} \left[\left(\frac{T_{nd,N} - T_{nd,P}}{\delta y_n} + \frac{T_{nd,P} - T_{nd,S}}{\delta y_s} \right) \Delta x \Delta y \Delta z \right] \tag{11}$$

The summation on the lefthand side of Eq. 11 includes all grid points in the solid phase of the RUC, and that on the righthand side include all grid points in the fluid phase of the RUC. The grid point designations P, N, and S, and the dimensions δy_s and δy_n, are shown with reference to the northern and southern finite volume boundaries in Figure 4.

Equilibrium and directional nonequilibrium thermal conductivities

With the T_e and T_{nd} temperature distributions known at all the grid points, it follows from Eqs. 8 and 9 that the equilibrium and directional nonequilibrium thermal conductivities can be calculated from

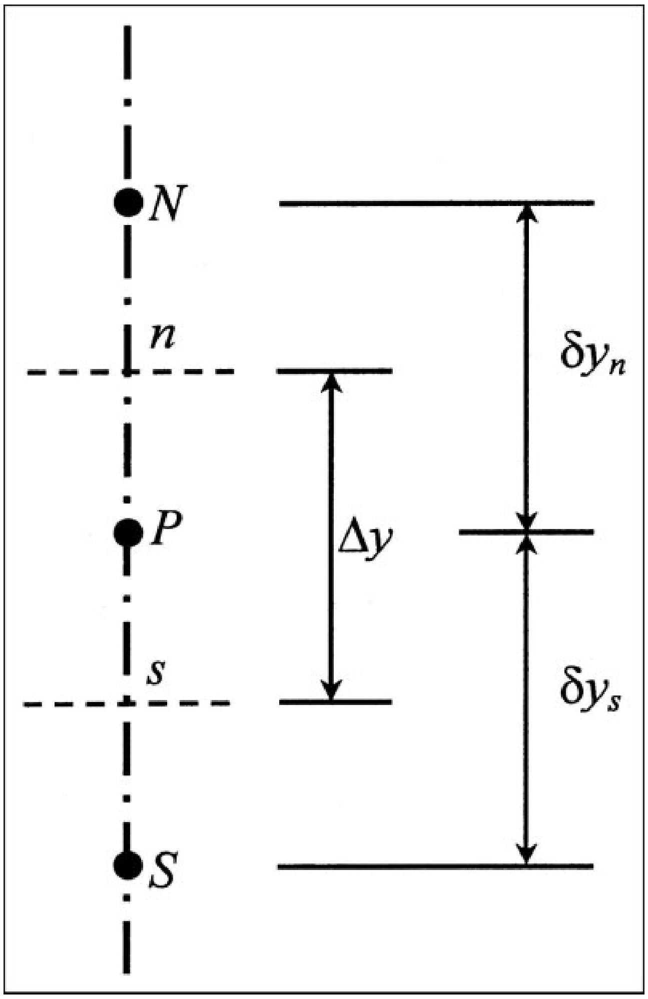

Figure 4. Finite volume.

$$k_{e/nd,\gamma} = \frac{d}{\varepsilon_\gamma(\bar{T}_{e/nd,\gamma,n} - \bar{T}_{e/nd,\gamma,s})} \times \frac{k_\gamma \sum_{V_\gamma} \left[\left(\frac{T_{e/nd,N} - T_{e/nd,P}}{\delta y_n} + \frac{T_{e/nd,P} - T_{e/nd,S}}{\delta y_s} \right) \Delta x \Delta y \Delta z \right]}{\sum_{V_s} \Delta x \Delta y \Delta z + \sum_{V_f} \Delta x \Delta y \Delta z} \tag{12}$$

where the subscript *e/nd* refers to either *e* or *nd*. The first term on the righthand side of Eq. 12 approximates the reciprocal of the gradients in the locally mean temperature given in the denominator of Eqs. 8 and 9, where d is the characteristic dimension of the RUC, as shown in Figure 2. Temperatures $\bar{T}_{e/nd,\gamma,n}$ and $\bar{T}_{e/nd,\gamma,s}$ are the mean boundary temperatures assigned at the northern and southern boundaries of the RUC, respectively. The solid and fluid phase volume fractions ε_s and ε_f are defined as

$$\varepsilon_\gamma \equiv \frac{V_\gamma}{V_o} \tag{13}$$

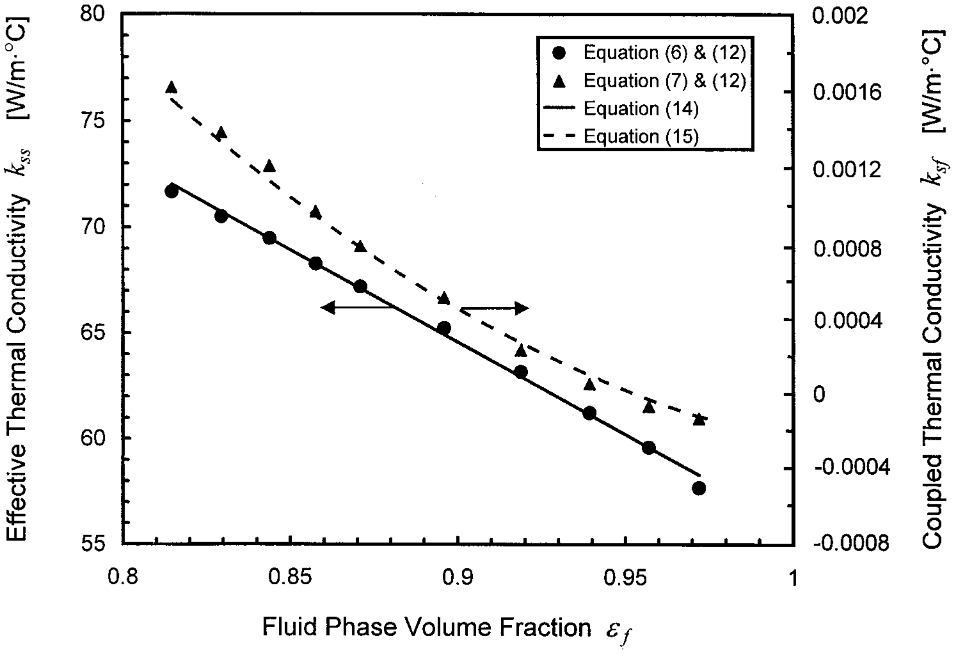

Figure 5. Solid-phase effective and coupled thermal conductivity for 6061 aluminum foam and air.

where $\gamma = s$ or f.

The resultant equilibrium and directional nonequilibrium thermal conductivities are independent of the arbitrarily selected temperatures assigned to the northern and the southern boundaries of the RUC.

Resultant correlations

Multiple sets of data for the equilibrium and directional nonequilibrium thermal conductivities were obtained in the manner discussed earlier. RUC properties were varied in the range: $0.8 < \varepsilon_f < 0.98$ and $0.0001 < k_f/k_s < 0.1$. Results for the effective and the coupled thermal conductivity of the solid and the fluid phase were determined from Eqs. 6 and 7, and correlated in terms of the thermal conductivity of the solid and fluid phases and the fluid phase volume fraction ε_f (generally referred to as porosity), by the following empirical expressions

$$\frac{k_{ss}}{k_s} = 0.559(1.64 - \varepsilon_f) + 0.562\,\frac{k_f}{k_s}\left(\frac{\varepsilon_f}{1 - \varepsilon_f}\right)^{0.235} \tag{14}$$

$$\frac{k_{sf}}{k_f} = 1.18\varepsilon_f^2 - 2.51\varepsilon_f + 1.32 \tag{15}$$

$$\frac{k_{ff}}{k_f} = 0.645(\varepsilon_f - 0.961)\,\frac{k_f}{k_s} + 1.82\varepsilon_f^2 - 3.29\varepsilon_f + 2.43 \tag{16}$$

and

$$\frac{k_{fs}}{k_s} = \left(\frac{k_f}{k_s}\right)^2(-14.2\varepsilon_f^2 + 22.6\varepsilon_f - 9.62) + 0.328\,\frac{k_f}{k_s}\left(\frac{\varepsilon_f}{1 - \varepsilon_f}\right)^{0.539} \tag{17}$$

Figures 5 and 6 show the solid and the fluid phase effective and coupled thermal conductivities for 6061 aluminum foam and air, a combination commonly used in the cooling of electronic devices (Antohe et al., 1996; Bastawros, 1998a; Lu et al., 1998a). The figures compare results from the numerical solutions of Eq. 10 to the correlations given in Eqs. 14 to 17. Comparisons with higher values of k_f/k_s (as high as $k_f/k_s = 1$) showed similar degrees of correlation than those presented in Figures 5 and 6.

Comparison between theory and experiment

Neither the effective and coupled thermal conductivities, nor the equilibrium and directional nonequilibrium thermal conductivities, can easily be evaluated through an experimental measurement. However, in Appendix B it is shown from the definitions of the effective, coupled and overall thermal conductivities that under thermal equilibrium conditions

$$\varepsilon_s k_{ss} + \varepsilon_f k_{sf} + \varepsilon_f k_{ff} + \varepsilon_s k_{fs} = k_o \tag{18}$$

Equation 18 allows the combination of parameters on the left to be compared to the experimental data for the overall thermal conductivity k_o on the right. Figure 7 shows experimentally determined data for the ratio k_o/k_f, from various sources, as a function of k_o/k_f, determined from Eqs. 14 to 18.

Also shown are data for k_o/k_f calculated from the analytical expression for the overall thermal conductivity of Calmidi and Mahajan (1999), for the combinations of 0.96-porosity nickel, aluminum, and RVC, with air, ethyl glycol, and water, respectively. Corresponding data obtained from the expressions for k_{ss} and k_{ff} of Calmidi and Mahajan (2002), used with Eq. 18, are also shown.

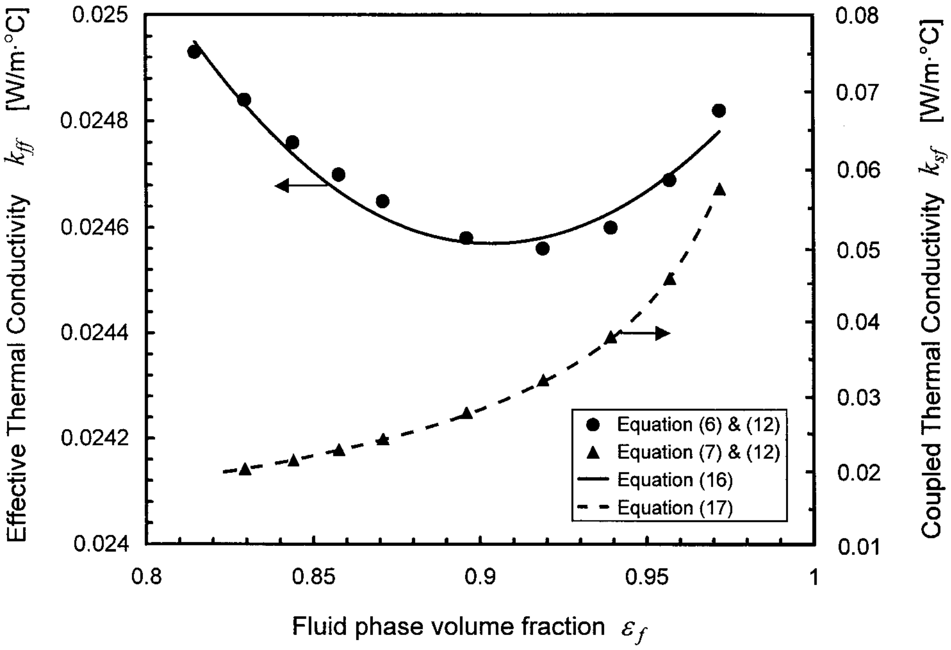

Figure 6. Fluid phase effective and coupled thermal conductivity for 6061 aluminum foam and air.

Discussion

Mathematical expressions were developed for the effective and the coupled thermal conductivity of open-cellular foams, presented in terms of the solid and fluid phase thermal conductivities and foam porosity. A method was used that defines the effective and the coupled thermal conductivity in terms of an equilibrium and a directional nonequilibrium thermal conductivity. The equilibrium and directional nonequilibrium thermal conductivities were determined by establishing an equilibrium and a directional nonequilibrium microscopic temperature distribution in a Representative Units Cell (RUC) for open-cellular foam, respectively. These microscopic temperature distributions were established through computation at a finite number of discrete grid points in the RUC.

The coupled thermal conductivity determines the effect of the locally mean temperature gradient in a particular phase on the actual locally mean conductive heat flux in the opposing phase. This effect is more profound in geometries with regions

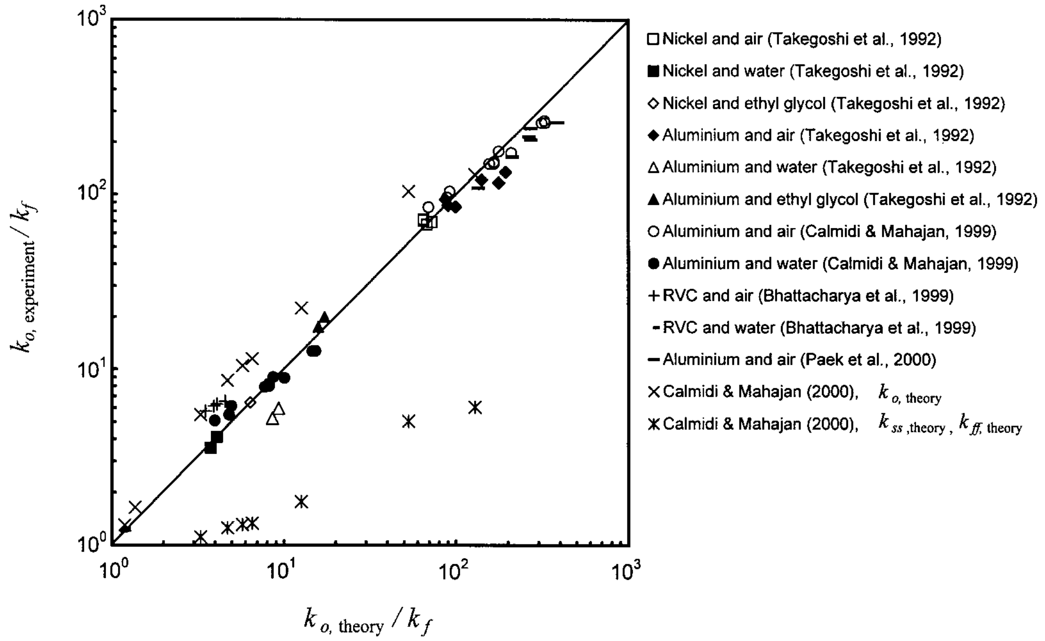

Figure 7. Experimental data for k_o/k_f as a function of k_o/k_f determined theoretically from this model.

where the two phases are geometrically composed in series with respect to the direction of conductive heat flow.

Tendencies observed in Eqs. 15 and 17 are consistent with the conclusions of Fourie and Du Plessis (2003), for porous media in general, in that the solid phase and the fluid phase coupled thermal conductivities both show a weak dependency on the solid phase thermal conductivity at low solid phase volume fractions.

The model used here does not take foam cell size into consideration in the calculation of the effective and coupled thermal conductivities of the solid and the fluid phase. Insensitivity of the overall thermal conductivity (related to the effective and coupled thermal conductivities through Eq. 18) to the foam cell size, is consistent with the experimental findings of Takegoshi et al. (1992) and Paek et al. (2000).

The combination of effective and coupled thermal conductivities given on the righthand side of Eq. 18, reduces to the overall thermal conductivity k_o in the case of thermal equilibrium between the solid and the fluid phase. This combination of the proposed model shows good correlation with experimental data. The analytical expression for the overall thermal conductivity k_o of Calmidi and Mahajan (2000) shows relatively good correlation with experimental data. However, virtually no correlation with experimental data is shown when expressions for k_{ss} and k_{ff} (Calmidi and Mahajan, 2000) are used with Eq. 18 to yield k_o. In fact, the combinations of RVC with ethyl glycol and RVC with water yielded values that were off the scale of Figure 7. Calmidi and Mahajan's expressions for k_{ss} and k_{ff} were obtained by setting k_s and k_f equal to zero in their analytical expression for the overall thermal conductivity, respectively. The resulting expressions analytically fail to satisfy the fundamental requirement given by Eq. 18, with k_{sf} and k_{fs} equal to zero.

Literature Cited

Ashby, M. F., A. Evans, N. A. Fleck, L. J. Gibson, J. W. Hutchinson, and H. N. G. Wadley, *Metal Foams - A Design Guide*, Butterworth-Heinemann (2000).

Antohe, B. V., J. L. Lage, D. C. Price, and R. M. Weber, "Numerical Characterization of Micro Heat Exchangers with Experimentally Tested Porous Aluminum Layers," *Int. J. of Heat and Fluid Flow*, **17**, 594 (1996).

Banhart, J., "Manufacturing Routes for Metallic Foams," *J. O. M*, **52**, 22 (2000).

Bastawros, A. F., "Effectiveness of Open-Cell Metallic Foams for High Power Electronic Cooling," *ASME Heat Transf. Division*, **361**, 211 (1998a).

Bastawros, A. F., A. G. Evans, and H. A. Stone, *Evaluation of Cellular Metal Heat Transfer Media*, Report MECH 325, Division of Engineering and Applied Sciences, Harvard University, Cambridge, MA (1998b).

Bauer, T. H., "A General Analytical Approach Toward the Thermal Conductivity of Porous Media," *Int. J. of Heat and Mass Transf.*, **36**, 4181 (1993).

Bear, J., and Y. Bachmat, "Macroscopic Modelling of Transport Phenomena in Porous Media: 2, Applications to Mass, Momentum and Energy Transport," *Transport in Porous Media*, **1**, 241 (1986).

Bhattacharya, A., V. V. Calmidi, and R. L. Mahajan, "Analytical-Experimental Study for the Determination of the Effective Thermal Conductivity of High Porosity Fibrous Foams," *ASME, Appl. Mech. Division*, **233**, 13 (1999).

Bird, R. B., W. E. Steward, and E. N. Lightfoot, *Transport Phenomena*, Wiley, New York (1960).

Calmidi, V. V., and R. L. Mahajan, "The Effective Thermal Conductivity of High Porosity Fibrous Metal Foams," *J. of Heat Transf.*, **121**, 466 (1999).

Calmidi, V. V., and R. L. Mahajan, "Forced Convection in High Porosity Metal Foams," *J. of Heat Transf.,* **122**, 557 (2002).

Carbonell, R. G., and S. Whitaker, "Heat and Mass Transfer in Porous Media," J. Bear and M.A. Corapcioglu, eds., *Fundamentals of Transport Phenomena in Porous Media*, Martinus Nijhof, 121 (1984).

Combarnous, M. A., and S. A. Bories, "Hydrothermal Convection in Saturated Porous Media," *Advances in Hydroscience*, **10**, 231 (1975).

Du Plessis, J. P., "Pore-Scale Modelling of Flow through Different Types of Porous Environments," *Heat and Mass Transfer in Porous Media*, M. Quintard and M. Todorovic, eds.,Elsevier, Amsterdam, 249 (1991).

Du Plessis, J. P., and J. H. Masliyah, "Mathematical Modelling of Flow Through Consolidated Isotropic Porous Media," *Transport in Porous Media*, **3**, 145 (1988).

Dul'nev, G. N., "Heat Transfer Through Solid Dispersed Systems," *Eng. Phy. J*, **9**,. 275 (1965).

Fortini A. J., and R. H. Tuffias, *Foam Heat Exchangers*, Report LEW-16579, NASA Lewis Research Center, Cleveland, OH (1998).

Fourie, J. G., and J. P. Du Plessis, "Pressure Drop Modeling in Cellular Metallic Foams," *Chem. Eng. Sci.*, **57**, 2781 (2002).

Fourie, J. G., and J. P. Du Plessis, "A Two-Equation Model for Heat Conduction in Porous Media - I: Theory," *Transport in Porous Media*, **33**, 145 (2003).

Gibson, L. J., and M. F. Ashby, *Cellular Solids*, Cambridge University Press, New York (1988).

Glatzmaier, G. C., and W. F. Ramirez, "Use of Volume Averaging for the Modelling of Thermal Properties of Porous Materials," *Chem. Eng. Sci.*, **30**, 3157 (1988).

Gray, W. G., "A Derivation of the Equations for Multiphase Transport," *Chem. Eng. Sci.*, 3**0**, 229 (1975).

Guilleminot, J. J., and J. M. Gurgel, "Heat Transfer Intensification in Adsorbent Beds of Adsorption Thermal Devices," *Proc. of Solar Eng.-The 12th Annual Int. Solar Eng. Conf.*, Miami, FL, ASME 69 (1990).

Hsu, C. T., "Modified Zehner-Schlunder Models for Stagnant Thermal Conductivity of Porous Media," *Int. J. of Heat and Mass Transfer*, **37**, 2751 (1994).

Hsu, C. T., "Closure Model for Transient Heat Conduction in Porous Media," *J. of Heat Transf.,* **121**, 733 (1999).

Hwang, J. J., G. J. Hwang, R. H. Yeh, and C. H. Chao, "Measurement of Interstitial Convective Heat Transfer and Frictional Drag for Flow Across Metal Foams," *J. of Heat Transf.,* **124**, 120 (2002).

Kamiuto, K., "Study of Dul'nev's Model for the Thermal and Radiative Properties of Open-Cellular Porous Materials," *JSME Int. J., Series B*, **40**, 577 (1997).

Kaviany, M., *Principles of Heat Transfer in Porous Media*, Springer-Verlag, New York (1995).

Kim, S. J., and S. P. Jang, "Effects of the Darcy Number, the Prandtl Number, and the Reynolds Number on Local Thermal Non-Equilibrium," *Int. J. of Heat and Mass Transfer*, **45**, 3885 (2002).

King, H. H., "A Poisson Equation Solver for Rectangular and Annular Regions," *Int. J. of Numerical Methods in Eng.*, **10**, 799 (1976).

Lu T. J., A. G. Evans, and J. W. Hutchinson, "The Effects of Material Properties on Heat Dissipation in High Power Electronics," *ASME J. of Electronic Packaging*, **120**, 280 (1998a).

Lu T. J., H. A. Stone, and M. F. Ashby, "Heat Transfer in Open-Cells Metal Foams," *Acta Materialia*, **46**, 3619 (1998b).

Moyne, C., "Two-Equation Model for a Diffusion Process in Porous Media using the Volume Averaging Method with an Unsteady-State Closure," *Advances in Water Res.*, **20**, 63 (1997).

Nozad, I., R. G. Carbonel, and S. Whitaker, "Heat Conduction in Multiphase Systems: I. Theory and Experiment for Two-Phase Systems," *Chem. Eng. Sci.*, **40**, 843 (1985).

Paek, J. W., B. H. Kang, S. Y. Kim, and J. M. Hyun, "Effective Thermal Conductivity and Permeability of Aluminum Foam Materials," *Int. J. of Thermophysics*, **21**, 453 (2000).

Patankar, S. V., *Numerical Heat Transfer and Fluid Flow*, Hemisphere, New York (1980).

Peng, H. X., Z. Fan, J. R. G. Evans, and J. J. C. Busfield, "Microstructure of Ceramic Foams," *J. of the European Ceramic Soc.*, **20**, 807 (2000).

Quintard, M., and S. Whitaker, "One- and Two-Equation Models for Transient Diffusion Processes in Two-Phase Systems,"*Advances in Heat Transf.*, **23**, 369 (1993).

Sathe, S. B., R. E. Peck, and T. W. Tong, "Numerical Analysis of Heat

Transfer and Combustion in Porous Radiant Burners," *Int. J. of Heat and Mass Transf.*, **33**, 1331 (1990).
Schlünder, E. U., "Equivalence of One- and Two-Phase Models for Heat Transfer Processes in Packed Beds: One-Dimensional Theory," *Chem. Eng. Sci.*, **30**, 449 (1975).
Schuetz, M. A., and L. G. Glicksman, "Basic Study of Heat Transfer Through Foam Insulation," *J. of Cellular Plastics*, **20**, 114 (1984).
Takegoshi, E., Y. Hirasawa, J. Matsuo, and K. Okui, "A Study on Effective Thermal Conductivity of Porous Metals," *Trans. of the Japanese Soc. of Mech. Eng.*, **58**, 879 (1992).
Tien, C. L., and K. Vafai, "Statistical Bounds for the Effective Thermal Conductivity of Microsphere and Fibrous Insulation," *AIAA Prog. Ser.*, **65**,. 135 (1979).
Twigg, M. V., and J. T. Richardson, "Theory and Applications of Ceramic Foam Catalysts," *Chem. Eng. Res. and Des.*, **80**, 183 (2002).
Vafai, K., and M. Sözen, "Analysis of Energy and Momentum Transport for Fluid Flow Through a Porous bed," *J. of Heat Transf.*, **112**, 690 (1990).
Viskanta, R., "Modeling of Transport Phenomena in Porous Media using a Two-Energy Equation Model," *Proc. of the ASME-JSME Thermal Eng. Joint Conf.*, **3**, 11 (1995).
Vortmeyer, D., and R. J. Schaefer, "Equivalence of One- and Two-Phase Models for Heat Transfer Processes in Packed Beds, One-Dimensional Theory," *Chem. Eng. Sci.*, **29**, 485 (1974).
Whitaker, S., "Diffusion and Dispersion in Porous Media", *AIChE J.*, **13,** 420 (1967).
Whitaker, S., "Simultaneous Heat, Mass and Momentum Transfer in Porous Media: A Theory of Drying," *Advances in Heat Transf.*, **13**, 119 (1977).
Whitaker, S., "Heat Transfer Catalytic Packed Bed Reactors," *Handbook of Heat and Mass Transfer*, 3, N.P. Cheremisinoff ed., Catalysis, Kinetics & Reactor Engineering, Gulf Publishers, Houston, TX (1989).

Appendix A: Characteristic Microscopic Temperature Distributions

Consider a principle direction denoted the direction y, which is collinear with the mean direction of conductive heat flow. The equilibrium temperature distribution T_e is a distribution that accounts for all directional conductive heat flow within a Representative Elementary Volume (REV) (Bear and Bachmat, 1986) in the principle direction y, such that the two phases are in complete thermal equilibrium *everywhere* within the REV. The net heat transferred across the interface between the two phases is, therefore, zero in the REV, that is

$$\int_{A_{sf}} (k\nabla T_e)_\gamma \cdot \boldsymbol{n}_{\gamma\varphi}\, \mathrm{d}A = 0 \tag{A1}$$

where $\gamma = s$ and $\varphi = f$, or *vice versa*.

Gray (1975) and Whitaker (1977) proposed that the net exchange of heat between the phases in a porous medium is directly proportional to the intrinsic volume-averaged temperature difference between the phases. The intrinsic volume-averaged equilibrium temperature of the solid phase is, therefore, equal to that of the fluid phase, that is

$$\frac{1}{V_s}\int_{V_s} T_e\, \mathrm{d}V = \frac{1}{V_f}\int_{V_f} T_e\, \mathrm{d}V \tag{A2}$$

and, because this condition is valid everywhere within the REV, it follows that, with reference to the direction y

$$\frac{\partial}{\partial y}\left(\frac{1}{V_s}\int_{V_s} T_e\, \mathrm{d}V\right) = \frac{\partial}{\partial y}\left(\frac{1}{V_f}\int_{V_f} T_e\, \mathrm{d}V\right) \tag{A3}$$

The directional nonequilibrium temperature distribution T_{nd} is a distribution that accounts for the directional conductive heat flow in the principle direction y within each phase in the REV, such that the net directional conductive heat flow in the principle direction y is zero, that is

$$\frac{k_s}{V_s}\int_{V_s} \frac{\partial T_{nd}}{\partial y}\, \mathrm{d}V = -\frac{k_f}{V_f}\int_{V_f} \frac{\partial T_{nd}}{\partial y}\, \mathrm{d}V \tag{A4}$$

The net exchange of heat between the two phases associated with T_n is also zero within the REV, that is

$$\int_{A_{sf}} (k\nabla T_{nd})_\gamma \cdot \boldsymbol{n}_{\gamma\varphi}\, \mathrm{d}A = 0 \tag{A5}$$

Again, with the hypothesis of Gray (1975) and Whitaker (1977), it follows that the intrinsic volume-averaged directional nonequilibrium temperatures of the solid and the fluid phase are equal *at the center* of the REV, that is

$$\frac{1}{V_s}\int_{V_s} T_{nd}\, \mathrm{d}V = \frac{1}{V_f}\int_{V_f} T_{nd}\, \mathrm{d}V \tag{A6}$$

Appendix B: Compatibility With A One-Equation Model

Consider a principle direction denoted the direction y, which is collinear with the mean direction of conductive heat flow. A two-equation model derived from the application of the analytical volume-averaging procedure (Whitaker, 1967; Bear and Bachmat, 1986) to the conduction terms of the energy equation, defines the effective and coupled thermal conductivities of the solid phase, such that (Quintard and Whitaker, 1993; Fourie and Du Plessis, 2003)

$$k_{ss} + k_{fs} \equiv \frac{\displaystyle\int_{V_s} \frac{\partial T}{\partial y}\, \mathrm{d}V}{\displaystyle\frac{\partial}{\partial y}\left(\int_{V_s} T\, \mathrm{d}V\right)} \tag{B1}$$

and those of the fluid phase, such that

$$k_{ff} + k_{sf} \equiv \frac{\displaystyle\int_{V_f} \frac{\partial T}{\partial y}\, \mathrm{d}V}{\displaystyle\frac{\partial}{\partial y}\left(\int_{V_f} T\, \mathrm{d}V\right)} \tag{B2}$$

Knowing that $\varepsilon_s = V_s/V_o$ and $\varepsilon_s = V_f/V_{o,}$ within a Representative Elementary Volume (REV) (Bear and Bachmat, 1986), it follows that

$$\varepsilon_s k_{ss} + \varepsilon_s k_{fs} + \varepsilon_f k_{ff} + \varepsilon_f k_{sf} = \frac{\dfrac{1}{V_o}\displaystyle\int_{V_s} \frac{\partial T}{\partial y}\,\mathrm{d}V}{\dfrac{1}{V_s}\dfrac{\partial}{\partial y}\left(\displaystyle\int_{V_s} T\,\mathrm{d}V\right)} + \frac{\dfrac{1}{V_o}\displaystyle\int_{V_f} \frac{\partial T}{\partial y}\,\mathrm{d}V}{\dfrac{1}{V_f}\dfrac{\partial}{\partial y}\left(\displaystyle\int_{V_f} T\,\mathrm{d}V\right)} \tag{B3}$$

With an assumption of thermal equilibrium between the solid and the fluid phase, it follows from Gray (1975) and Whitaker (1977) that

$$\frac{1}{V_s}\int_{V_s} T\,\mathrm{d}V = \frac{1}{V_f}\int_{V_f} T\,\mathrm{d}V = \frac{1}{V_o}\int_{V_o} T\,\mathrm{d}V \tag{B4}$$

Substituting Eq. B4 into Eq. B3, and noting that $V_s + V_f = V_o$ yields

$$\varepsilon_s k_{ss} + \varepsilon_s k_{fs} + \varepsilon_f k_{ff} + \varepsilon_f k_{sf} = \frac{\displaystyle\int_{V_o} \frac{\partial T}{\partial y}\,\mathrm{d}V}{\dfrac{\partial}{\partial y}\left(\displaystyle\int_{V_o} T\,\mathrm{d}V\right)} \tag{B5}$$

The righthand side of Eq. B5 is the classic definition of the overall thermal conductivity k_o in a one-equation model, for thermal conduction at a macroscopic level in a porous medium with thermal equilibrium between the two phases (Nozad et. al., 1985).

Manuscript received May 7, 2003, revision received June 26, 2003, and final revision received Dec. 18, 2003.